AUTHORS' POSTPRINT Originally published in AIP Conference Proceedings 2156, 020011 (2019); https://doi.org/10.1063/1.5125876

Direct contact plating - Inline plating solution for ZEBRA IBC by local contacting

Katharina Gensowski[1, a)], Gisela Cimiotti[1], Jonas Eckert[1], Varun Arya [1], Juan Garcia la Roche[1], Julien Scheffelmeier[1], Bastien Decker[1], Giuseppe Galbiati[2], Dominik Rudolph[2] and Sven Kluska[1]

[1]Fraunhofer Institute for Solar Energy Systems ISE, Heidenhofstraße 2, 79110 Freiburg im Breisgau, Germany
[2]International Solar Energy Research Center Konstanz e.V., Rudolf-Diesel-Straße 15, 78467 Konstanz, Germany

[a)]Corresponding author: katharina.gensowski@ise.fraunhofer.de

Abstract. An inline plating solution, in which electrolyte and contact system are arranged on the same side, is presented in this work. This concept allows plating onto cell concepts that do not have existing seed metallization on a significant share of surface area, e.g. ZEBRA IBC solar cell. Local contacting of Si or local metal structures is required to enable plating on these cell concepts. A new contacting scheme, which includes a stainless steel brush, was adapted into the existing inline plating tool of the company RENA Technologies GmbH. It allows local contacting of Si and of metal structures without any temporary masking. First results of a plated contact grid on a ZEBRA IBC solar cell are successfully demonstrated. One result presents the simultaneous plating of n-type BSF and p-type emitter with finger heights of 18 µm ± 2 µm and of 10 µm ± 1 µm, respectively. In addition, important process development steps such as alignment are shown. An edge inhomogeneity and simultaneous plating on both polarities could be solved by introducing an electroless Ni seed. Furthermore, a plating voltage limitation proved also to be beneficial for plating homogeneity. Adaptations in the inline plating tool were also made.

INTRODUCTION

Until now, the interdigitated back-contact (IBC) solar cell concept is not widely established in the industrial market, though this cell concept has got the potential of highest efficiency. 26.7% was presented by Kaneka *et al.* for a heterojunction back contact solar cell [1]. One of the main challenges of IBC solar cells is to lower production costs for metallization, as described by NREL [2]. Metallized contacts on IBC solar cells are commonly realized by screen printing [3]. Instead of developing new processes, established process sequences can be simplified in their complexity in order to lower metallization costs. So far, IBC solar cells have been plated in mass production by SunPower [4, 5]. A temporary masking of the IBC solar cell is required. In this work plating without temporary mask for ZEBRA IBC solar cells is presented as another possibility to reduce production costs for metallization. For this purpose, existing industrial inline plating systems of the company RENA Technologies GmbH are used and modified with regard to the contacting system.

To generate maskless plating on ZEBRA IBC solar cells, several requirements have to be realized and some challenges have to be solved.

- Alignment of laser ablation onto n-type and p-type doped areas
- Local contacting of Si or of metal structures

- Simultaneous metallization of n-type doped vs. p-type doped regions
- Finger height homogeneity / edge homogeneity / finger conductivity
- Low contact resistivity
- Strong finger adhesion

The alignment of laser ablation on boron and phosphorous diffused areas is no problem technologically with today's laser systems. The second aspect, local contacting of Si or of metal structures to realize a plated contact grid, was one of the biggest challenges in our work. There was no contact system for such microstructures available. In this work, we developed such a contact system with brushes.

The simultaneous plating on n-type doped and p-type doped areas was already shown by Goa *et al.* and Tous *et al.*, but especially the plating on p-type doped regions is quite challenging [6, 7, 8]. Theoretically, a homogeneous plating result concerning the finger height is possible. It will be shown in this work, that this was a big issue with the chosen setup and settings. The finger height homogeneity can be achieved within certain limits. Good cell results require low contact resistivity and strong finger adhesion. It is known from literature that plated contacts on n-type doped and p-type doped areas have low contact resistances [9, 10]. Kluska *et al.* presented that a strong finger adhesion can be expected by using a ps-laser system and textured surfaces [10]. A rough surface is generated.

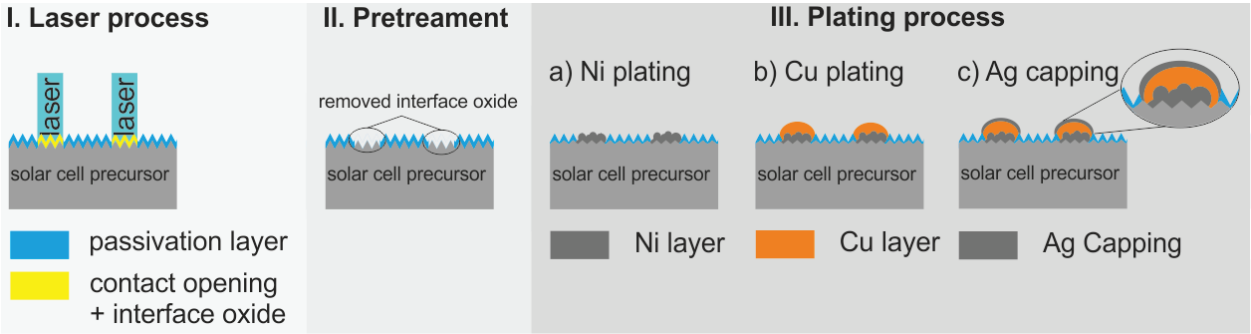

FIGURE 1. Plated metal contacts on ZEBRA IBC solar cells can be realized by combination of laser ablation and wet chemical metal deposition. (I) The contact grid is defined via local laser ablation of the passivation layer. (II) The pretreatment provides an HF-dip to remove laser induced and native oxide layer within the laser opening. (III) A Ni seed layer is plated onto the laser-opened area. Subsequently Cu is plated onto the Ni seed. The metal stacks of the plated structures are capped by a thin Ag layer (< 0.5 µm).

The metallization of ZEBRA IBC solar cells requires conductive metal fingers with low contact resistances to n-type and p-type doped surfaces. The application of plated Ni/Cu/Ag fulfills these requirements and enables the possibility to lower material costs compared to Ag-screen printing. The used process route to create plated contact fingers on solar cells at Fraunhofer ISE is shown in Fig. 1. The n-type and p-type doped contact areas are defined by local laser ablation of the passivation layer. To remove oxide layers in the laser patterned openings, a pretreatment with hydrofluoric acid (HF) is done. Subsequently, Ni, Cu and Ag are plated onto the laser-opened areas [10]. The Ni layer acts as diffusion barrier to prevent diffusion of the copper into silicon. The main conducting material is the Cu layer. To realize the interconnection of the ZEBRA IBC solar cells the Ag capping is required. Optionally, an annealing step can follow to improve the adhesion of the plated structures on silicon by forming silicides in the interface of silicon and Ni [11, 12].

So far, inline plating solutions are focusing on solar cell concepts with a full-area metallized rear side, e.g. passivated emitter and rear cell (PERC) [5]. The applied inline plating solution in the work of Horzel *et al.* uses an inline plating tool, which allows a single side immersion of the solar cell in the plating electrolyte. The seed metallization is kept dry during the plating process and is used for contacting to apply the process current.

This work demonstrates one process solution to enable plated Ni/Cu/Ag metallization for cell concepts where no seed metallization on a significant share of surface area is available during plating, such as IBC solar cells. Existing inline plating systems, which are usually used for PERC solar cell metallization, are modified to realize the plating processes of Ni/Cu/Ag on ZEBRA IBC solar cells. The technical solution of the contacting system for ZEBRA IBC solar cells as well as the proof-of-principle of this idea will be demonstrated on 156 x 156 mm² n-type Cz-silicon based solar cells.

EXPERIMENTAL

Approach

The scheme in Fig. 2a shows schematically an inline plating tool for PERC solar cells of the company RENA Technologies GmbH. Plating of metals is realized by reduction of positively charged metal ions from a chemical solution (electrolyte), which is possible by providing electrons from an external current [13]. The electrical contact during plating is provided by brushes on the metallized solar cell rear side. An image section of the contact brush is shown in Fig. 3a. The plating deposition is realized in the electrolyte on the opposite side of the solar cell. That means that the dry metallized side is contacted by using brushes and the side facing the electrolyte is plated when current is applied. The rolls move the solar cells through the inline plating tool. This simple inline tool concept, especially the contact system, has been modified to realize the inline plating process on ZEBRA IBC solar cells [14, 15, 16].

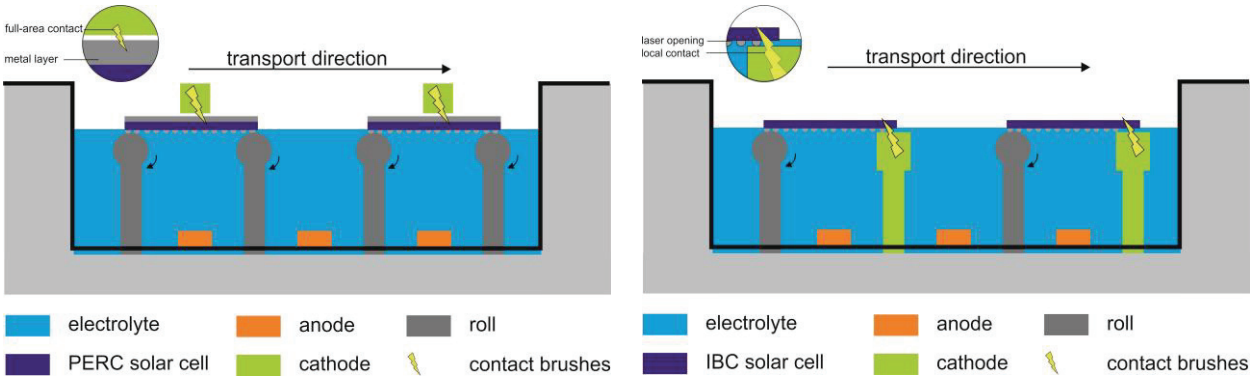

(a) (b)

FIGURE 2. Inline plating system. (a) Setup for plating on PERC cells. Contact system and electrolyte are on opposite sides of the solar cell. Brushes of contact system contact the metallized solar cell rear side. (b) Setup for local, direct plating on ZEBRA IBC solar cells. Contact system and electrolyte are on the same side. The cathode is realized with syphons, which contain brushes to transport the process current.

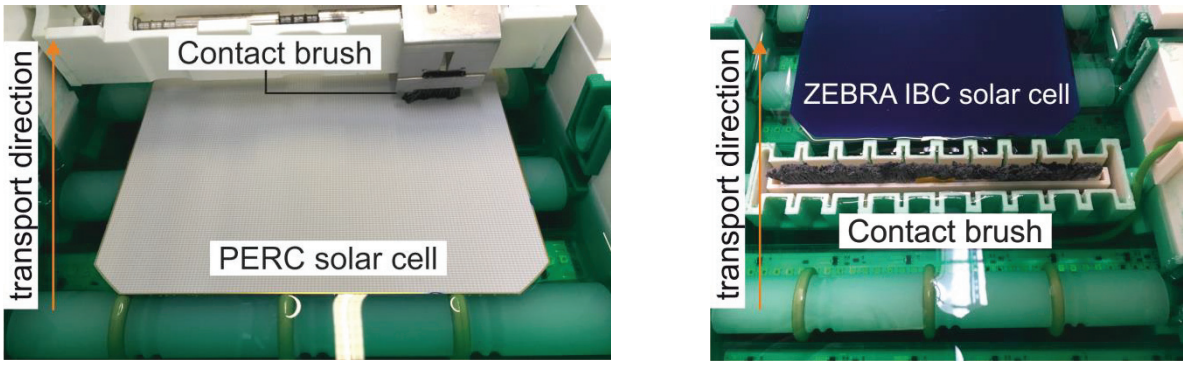

(a) (b)

FIGURE 3. Image section of Ni inline plating system. (a) Set-up for plating PERC solar cells. The contact brush places the process current onto the metallized layer (full-area contact). (b) Device for plating ZEBRA IBC solar cells. The contact brush has to apply the process current onto the electrolyte-wetted cell surface (local, direct contacts of Si or metal structures).

To achieve the local, direct contact plating onto ZEBRA IBC solar cells, the contact system and electrolyte have to be on the same side (Fig. 2b). The contact brushes are capable to provide electrical contact with the silicon surface within the laser contact openings. Local, direct contact plating allows the fabrication of plated Ni seed layers to enable low contact resistivities on p-type and n-type doped surfaces. Furthermore, plated Cu allows high finger conductivity. The developed tool concept allows Ni and Cu deposition onto the laser-opened contact grid.

In Fig. 3b the adaptation of the inline plating tool of the company RENA Technologies GmbH is imaged (scheme Fig. 2b). The Ni electrolyte wets the solar cell side with the contact grid. The contact grid is plated, when the cell touches the syphon's brushes. The syphons are 3D-printed with the polymer acrylonitrile styrene acrylate (ASA) and contain stainless steel brushes (Fig. 4). The syphon has got a width of 44 mm and a length of 170 mm. The contact brush covers the whole wafer width of a 156 x 156 mm² ZEBRA IBC solar cell. The geometry of the syphon is similar to that of ribs, this ensures that the cell surface and the electrolyte are in contact with each other as long as possible. There is no electrolyte directly next to the contact brush, in this zone the cell surface cannot be wetted by the electrolyte.

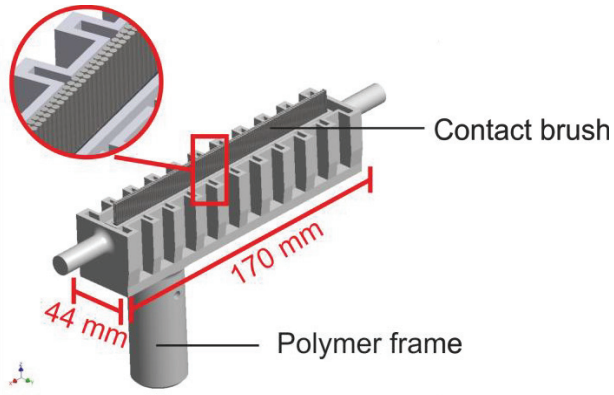

FIGURE 4. 3D-drawing of contact system to plate ZEBRA IBC solar cells by local contacting. The frame of the contact system (syphon) is produced by 3D-printing of ASA polymer. The frame is 44 mm wide and 170 mm long. The geometry of the syphons is similar to ribs. The stainless steel brushes are included in the center of the frame to apply the process current to the solar cell.

ZEBRA IBC Solar Cells

ZEBRA IBC solar cell precursors, as described in [15, 16], are processed for creating a plated metallization following the process sequence in Fig. 1 by using the adaption of the inline plating tool showed in Fig. 2b. The laser ablation is done with a ps-pulsed UV laser to structure the contact grid by local removal of the silicon nitride passivation layer. Using a ps-pulsed UV laser ensures adhesion due to the rough surface topography [10]. The contact grid consists only of fingers, no busbars are lasered.

To remove the native oxide layer in the lasered contact grid a pretreatment of 30 s HF dip is applied. The Ni seed layer is manufactured in two process steps. An electroless Ni electrolyte to deposit Ni seeds containing 1% phosphorous on the laser opened areas is used first, followed by an electroplated Ni layer. The electroless Ni electrolyte is an ammonia-containing electrolyte with a pH of 9.6 and an operating temperature of 88°C. The electroplated Ni electrolyte is operated at 50°C and at pH of 4.0. The applied current is 185 mA (depending on opened laser grid area) and the voltage is limited to 5 V.

The nitric acid-based copper electrolyte has a pH smaller than 0 and a working temperature of 30 °C. The used current is 340 mA with a limitation of 5 V (depending on opened laser grid area). Ag capping is carried out with an electroless electrolyte by exchanging Cu atoms for Ag atoms.

n-type Cz-silicon wafers with the dimensions of 156.75 x 156.75 mm² and a diameter of 210 mm are used. n-type doped and p-type doped areas alternate next to each other [15, 16]. The surface doping concentration N_s is 1.5×10^{20} cm^{-3} for the n-type doped areas and 1.5×10^{19} cm^{-3} and 4.0×10^{19} cm^{-3} for the p-type doped areas, respectively. Each polarity has 109 or 110 fingers, respectively, with a laser opening width of 12 µm.

RESULTS AND DISCUSSION

The requirements to realize the direct inline plating on ZEBRA IBC solar cells with local contacts were listed in the introduction of this work. In this section the different requirements are discussed concerning their realization and if necessary concerning their challenges and solutions.

Alignment

To realize plating contacts on ZEBRA IBC solar cells, a lasered contact grid on boron and phosphorous diffused areas is required. Only fingers have to be created in this case. The used ps-pulsed UV laser has to be aligned onto the n-type and p-type doped areas of the ZEBRA IBC solar cell. The n-type doped area is 400 µm wide. The width of the p-doped area is 900 µm. The laser-opened contact grid can be aligned in each case in the middle of the alternated regions (Fig. 5). Depending on the chosen laser energy the laser-opened fingers are 10 µm to 15 µm wide.

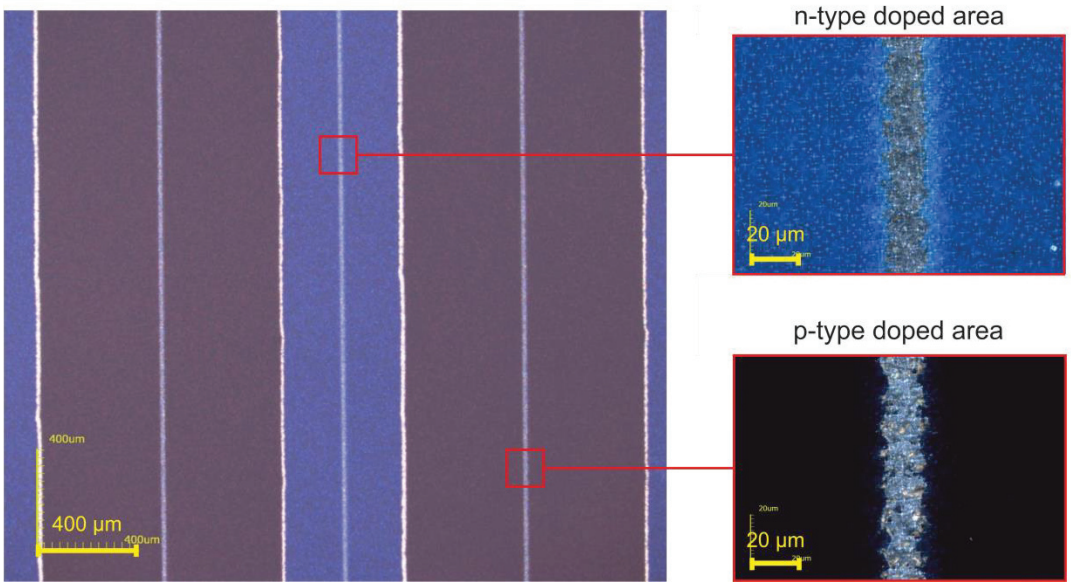

FIGURE 5. Confocal microscope images of the alternated n-type and p-type doped regions with laser-aligned contact of ZEBRA IBC solar cell. The laser-opened fingers are 10 µm to 15 µm wide.

Contacting of Local Si or Metal Structures

Figure 6 illustrates an electroplated Ni layer on laser-opened contact grid. Electroplated Ni deposition is obtained on both n-type doped and p-type doped area, which was achieved by the direct local contact of silicon. It was found that deposition to phosphorous diffused (h_{finger} 3 µm) areas was preferred to boron diffusion areas (h_{finger} > 1 µm) on the ZEBRA IBC solar cell. A Ni electrolyte with modified properties and a local contacting system makes it possible to achieve Ni plating on silicon.

To create a more homogeneous Ni layer and to ensure simultaneous plating on n-type and p-type doped areas, the Ni deposition can also be realized in two process steps - the electroless Ni seed deposition and the electroplated Ni deposition. The contact resistivity between electroless Ni seeds and contact brushes should in principle be lower compared to silicon. Figure 7 shows a successful deposition of electroless Ni seeds containing 1% phosphorous on n-type doped and p-type doped areas of a ZEBRA IBC solar cell. The SEM images present the typical rounded shape of Ni seeds. The clear boundary between laser-opened areas and the non-laser-opened passivation layer can be identified by Ni seed deposition (Fig. 7b und 7d). Electroless Ni seeds are deposited on the laser-opened contact grid.

Figure 8 depicts confocal images of the Ni stack from both electroless and electroplating deposition on phosphorous diffusion (Fig. 8a) and on boron diffusion (Fig. 8b). The improved contact between the contact brush

and the electroless Ni seeds allows an optimized electroplated Ni deposition on p-type doped areas. The finger height of this Ni layer is 1 µm. On n-type doped areas the finger height is 4 µm. However, the finger heights differ still between both diffusion regions. This phenomenon is not fully understood yet.

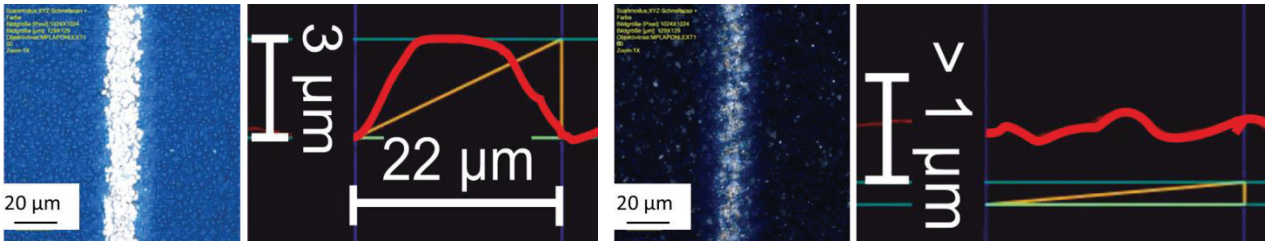

(a) (b)

FIGURE 6. Confocal microscope images of the alternated n-type (a) and p-type (b) doped regions with electroplated Ni deposition of ZEBRA IBC solar cell (1000 x). Plating is preferred on n-type doped regions compared to p-type doped regions.

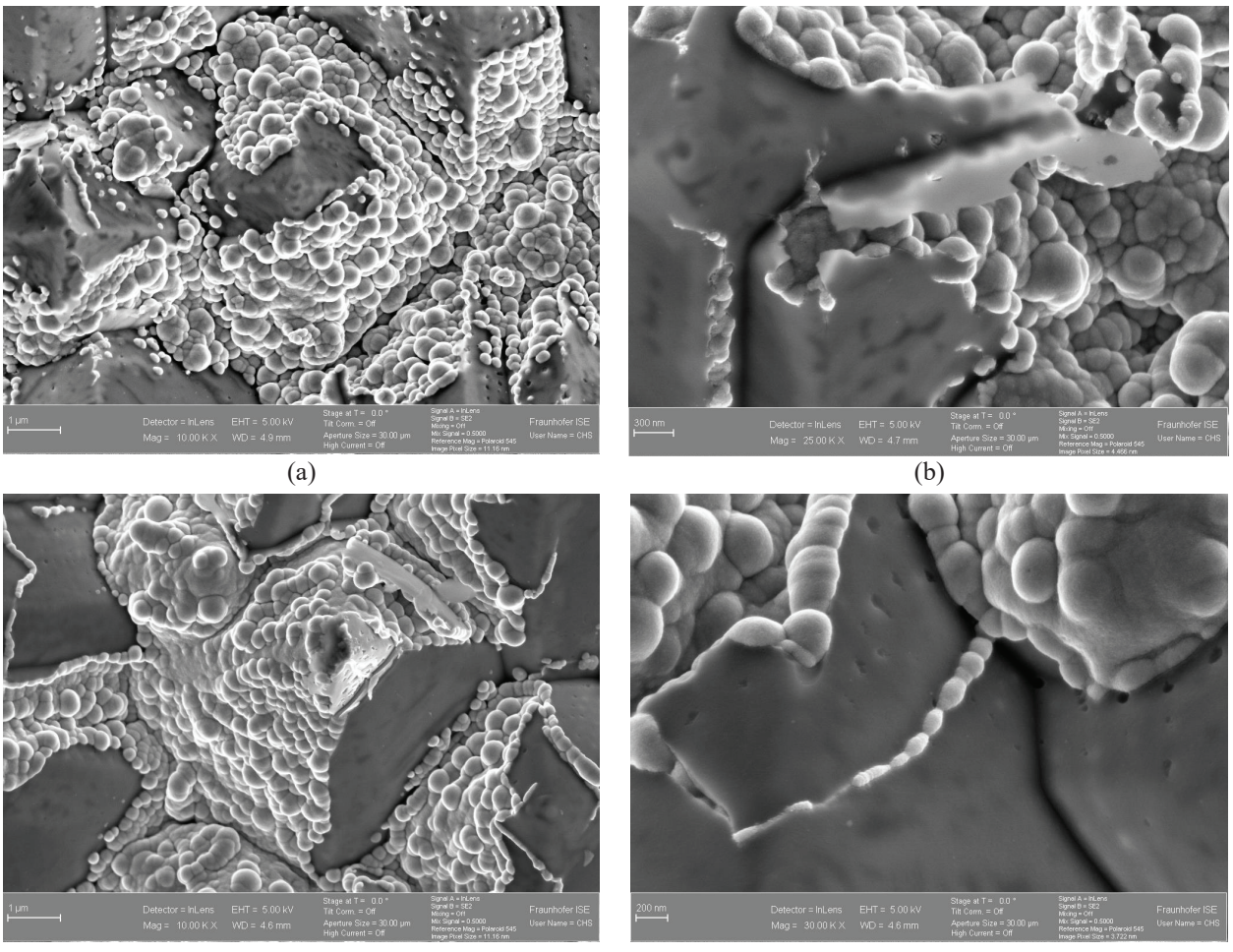

(a) (b)

(c) (d)

FIGURE 7. SEM characterization of electroless Ni seeds on laser-opened contact grid of ZEBRA IBC solar cell. (a) Ni seeds on pyramid in n-type doped area. (b) Ni seeds are located on laser-opened area, the non-laser-opened area have no Ni seeds (n-type doped area). (c) Ni seeds on pyramid in p-type doped area. (d) Ni seeds are located on laser-opened area, the non-laser-opened area have no Ni seeds (p-type doped area).

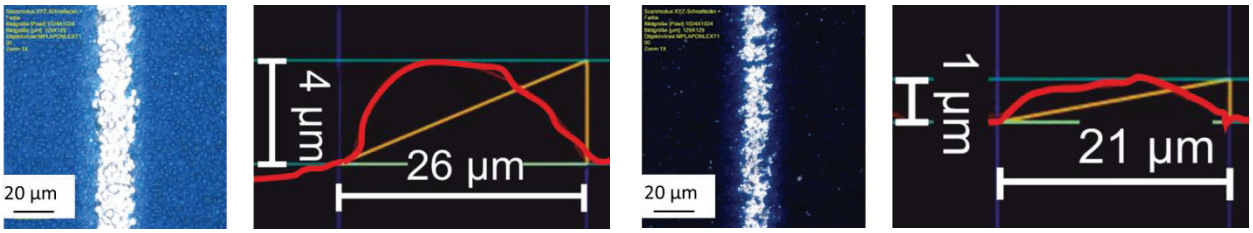

(a) (b)

FIGURE 8. Confocal microscope images of the alternated n-type (a) and p-type (b) doped regions with electroless Ni and electroplated Ni deposition of ZEBRA IBC solar cell (1000 x). Plating is still preferred on n-type doped regions compared to p-type doped regions.

Simultaneous p-type vs. n-type Metallization

It is quite challenging to achieve simultaneous plating on ZEBRA IBC solar cells, which means to plate on n-type doped and p-type doped areas on the cell rear side at the same time. Both regions are not on the same z-axis level due to differences in front-end processing and also the contact resistivity might differ. n-type doped areas are preferably plated. To ensure the simultaneous plating on ZEBRA IBC solar cells, the deposition of electroless Ni seeds onto the contact grid is needed. In addition, the deposition of electroless Ni seeds lowers the inhomogeneity of finger heights between n-type doped and p-type doped regions.

Finger Height Homogeneity/ Edge Homogeneity/ Finger Conductivity

When the electroplated Ni layer is deposited with an applied current and with maximum 32 V (no voltage limitation), the plating result is inhomogeneous concerning finger height and edge homogeneity. Upon first contact of the brush with the wafer, the voltage rapidly increases to 32 V. This is due to the high resistance for the plating current to reach a portion of wafer surface with wetted electrolyte. Heat might be produced which causes an evaporation of the Ni electrolyte on parts of the cell surface. Then, the voltage enormously decreases again and approaches a constant voltage value (horizontal asymptotic curve) during the remaining plating process. To realize a more homogeneous metallic deposition and a lower resistance for current spreading, the process sequence is extended by the electroless Ni seed deposition. But even in this case, if the voltage in the subsequent electroplating process is not limited, the deposition is still inhomogeneous. The same sharp voltage increase is observed, leading to inhomogeneity at the edge. Also, the finger height differs significant between n-type doped and p-type doped areas.

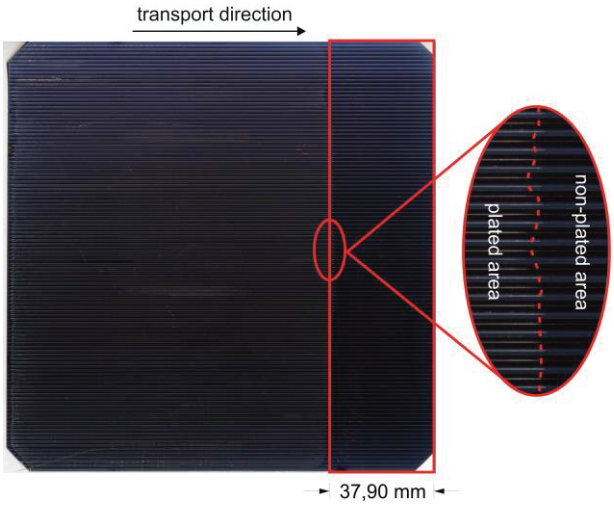

FIGURE 9. Edge inhomogeneity, non-plated area. Non-plated area results of the first contact of contact brush and ZEBRA IBC solar cell.

Finally, the successful direct contact plating sequence developed in this work consists of electroless Ni seed deposition and electroplated Ni deposition with a voltage limitation. A reasonable voltage limitation has been found to be 5 V, which still allows the applied current to be reached. The edge homogeneity can be realized in this case. To reduce the finger height difference between n-type and p-type doped areas again and to guarantee a locally good contact between contact brush and solar cell, the contact pressure is adjusted in the plating process. This pressure is realized with a countering force on top of the ZEBRA IBC solar cell. If the contact pressure is too high, the plated fingers are removed by brushes of the syphons because of too high mechanical stress.

The edge inhomogeneity is an effect that originates from the first syphon in the Ni electrolyte, where the first contact area of the ZEBRA IBC cell in transport direction is not plated on n-type doped and p-type doped areas (Fig. 9). If the edge inhomogeneity has been formed during the first contact with the brush, this area is no longer plated during the entire plating process. Our hypothesis is that the contact resistance of this non-plated area is too high compared to the remaining seeded contact grid because of a possible surface modification e.g. oxidation. The non-plated area of the ZEBRA IBC cell corresponds either to the half width or the whole width of the syphon. This non-plated area results as well in an inhomogeneous plating outcome.

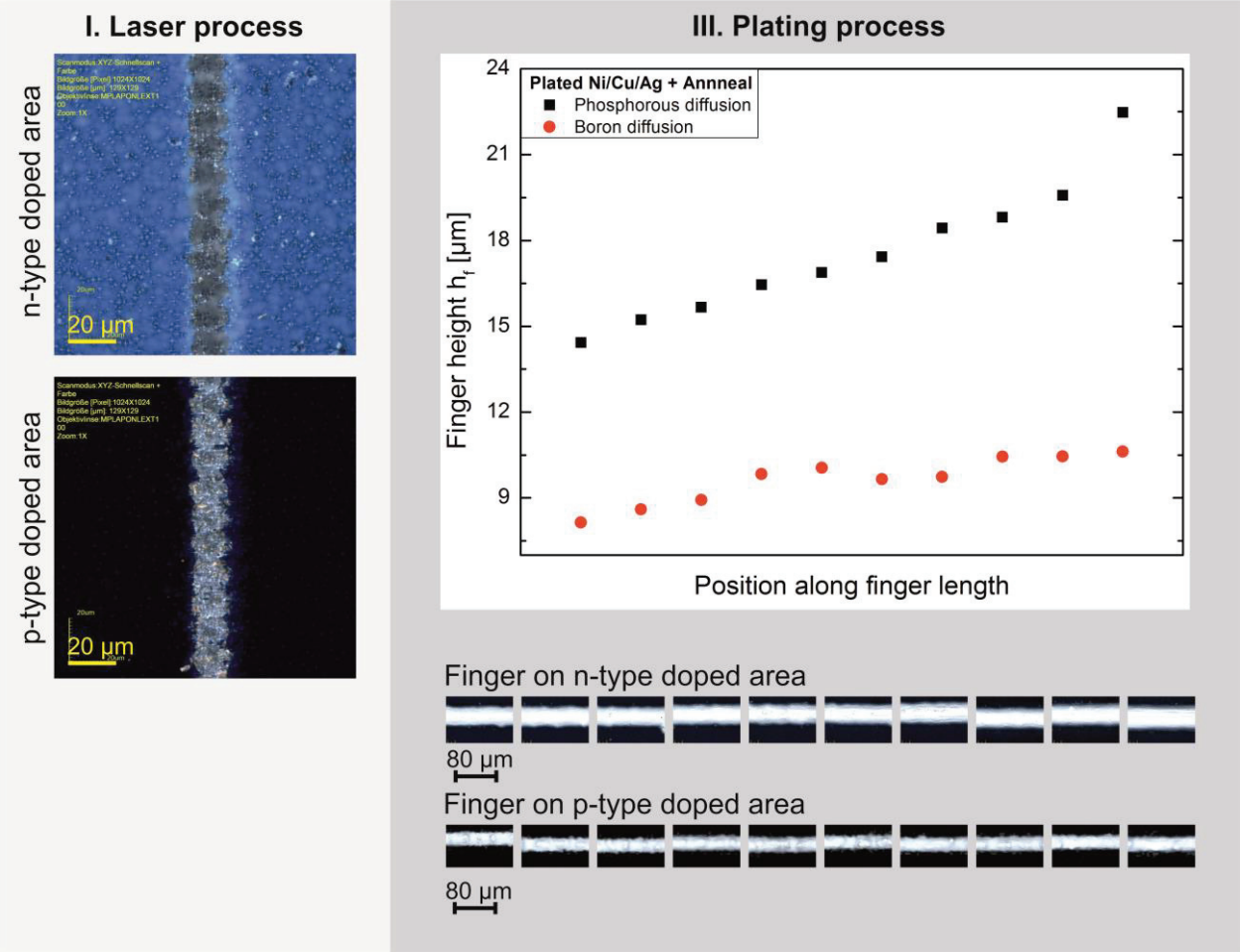

FIGURE 10. Plating result of 156 x 156 mm² ZEBRA IBC solar cell. Confocal microscope images (1000 x) of the laser opening of n-type doped and p-type doped areas (left). Confocal microscope images (1000 x) of Ni/Cu/Ag plated finger on n-type doped and p-type doped areas (right). The diagram illustrates the measured finger heights of the plated structures. The average height on n-type doped area is 18 µm ± 2 µm, the average height on p-type doped area is 10 µm ± 1 µm.

The local, direct contact plating process of Fig. 2b was demonstrated successfully on 156 x 156 mm² ZEBRA IBC solar cells. Figure 10 shows exemplary confocal microscope-images of the laser contact openings as well as

confocal microscope-images after the inline plating process that had been set to obtain plating heights of Ni(1-3 µm)/Cu(10-15 µm)/Ag(0.5 µm).

Confocal microscope-images were taken along the full finger length of 156 mm. The plated finger heights on n-type doped area vary from 14 µm to 22 µm. On average, the height of 18 µm ± 2 µm and the width of 48 µm ± 3 µm were measured. The aimed height of 15 µm to 20 µm on phosphorus diffusion is reached. The values on p-type emitter range from 8 µm to 11 µm. The average height of the plated fingers is 10 µm ± 1 µm, the average width is 41 µm ± 3 µm. Generally, plating on n-type BSF is preferred. Further process optimizations aim to equalize the height ratio of p-type doped and n-type doped metallized fingers.

It has been shown that it is possible to obtain thick plated contact fingers on ZEBRA IBC solar cells. The homogeneity of the layer thickness has to be improved. One observed effect is that the finger height increases along the wafer length. Also, the finger height differs between n-type and p-type doped areas. Still with the obtained metal distribution series resistance limitations should be kept at a low level. It is worthy to mention that quite narrow fingers with high conductivity could be created, which are well suited also for bifacial light collection.

Contact Resistivity

Transmission line measurements of plated Ni/Cu/Ag lines on different phosphorous doped and boron doped profiles were performed. The chosen doping profiles were developed at the ISC Konstanz for the application in ZEBRA IBC solar cells. The sheet resistance of the profiles varied between 20 Ω/sq. and 100 Ω/sq. The metallization sequence was similar to the samples shown in Fig. 10. Low contact resistivities of less than 1 mΩcm² could be demonstrated on both p-type doped and n-type doped surfaces. The results are shown in Fig. 11.

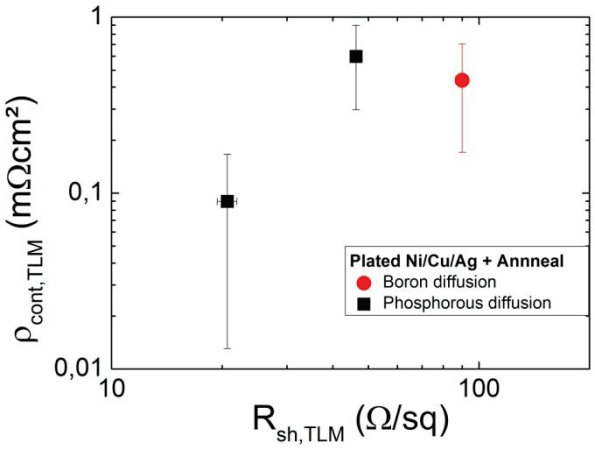

FIGURE 11. Contact resistivity results of direct contact plated fingers on boron diffusion and phosphorous diffusion surfaces. The predefined surface doping concentrations N_s were determined by electrochemical capacitance voltage (ECV) measurements on reference samples. N_s is $2.4x10^{19}$ cm^{-3} to $1.1x10^{20}$ cm^{-3}.

CONCLUSION

By combining an industrial inline plating tool and rapid prototyping, we could achieve a simple, adapted inline plating tool to realize direct inline plating on local contacts of ZEBRA IBC solar cells without using any temporary mask. In this approach the contact system and the electrolyte are on the same side. All defined requirements for a successful metallization could be reached. Electroless Ni seeds ensure simultaneous plating on the contact grid of the ZEBRA IBC solar cells. The next steps will be to measure the finger adhesion quantitatively and to demonstrate the first efficiencies of ZEBRA IBC solar cells. Additionally, the interconnection will be realized by using the multi-layer metallization concept [17]. So far, the results indicate that direct inline plating can be an alternative metallization process for ZEBRA IBC solar cells to simplify a plated process sequence and potentially to lower metallization costs while offering efficiency increase potential, which could make ZEBRA IBC solar cells more

economic for the industrial market. Additionally, this technology has the potential to be used for metallization of bifacial solar cell concepts.

ACKNOWLEDGEMENTS

This work was funded by the German Federal Ministry for Economic Affairs and Energy within the project "5CT", grant No. 0324092B and by the European project NEXTBASE under the European Union's Horizon 2020 research and innovation program under grant agreement no. 727523.

REFERENCES

1. M. A. Green *et al.*, "Solar cell efficiency tables (version 50)," *Prog. Photovolt: Res. Appl*., vol. 25, no. 7, pp. 668-676, 2017.
2. National Renewable Energy Laboratory, Silicon Materials and Devices R&D, Photovoltaic Research NREL. [Online] https://www.nrel.gov/pv/silicon-materials-devices-rd.html (Available: Accessed on April 25 2019).
3. G. Galbiati *et al.*, "Results on n-type IBC solar cells using industrial optimized techniques in the fabrication processing," *Energy Procedia*, vol. 8, pp. 421–426, 2011.
4. G. Harley *et al.*, (Sunpower Corporation), "US 2018 / 0254360 A1 Metallization of solar cells," 2018.
5. J. T. Horzel *et al.*, "Industrial Si solar cells with Cu-based plated contacts," *IEEE J. Photovoltaics*, vol. 5, no. 6, pp. 1595–1600, 2015.
6. J.-H. Guo *et al.*, "19.2% efficiency n-type laser-grooved silicon solar cells," *IEEE J. Photovoltaics*, pp. 983–986, 2005.
7. J.-H. Guo *et al.*, "Metallization improvement on fabrication of interdigitated backside and double sided buried contact solar cells," *Solar Energy Materials and Solar Cells*, vol. 86, no. 4, pp. 485–498, 2005.
8. L. Tous *et al.*, "22.4% bifacial n-Pert cells with Ni/Ag co-plated contacts and Voc ~691 mV," *Energy Procedia*, vol. 124, pp. 922–929, 2017.
9. F. Feldmann *et al.*, "Evaluation of Topcon technology on large area solar cells," *33rd European Photovoltaic Solar Energy Conference and Exhibition*, pp. 465–467, 2017.
10. S. Kluska *et al.*, "Electrical and mechanical properties of plated Ni/Cu contacts for Si solar cells," *Energy Procedia*, vol. 77, pp. 733–743, 2015.
11. A. Mondon *et al.*, "Microstructure analysis of the interface situation and adhesion of thermally formed nickel silicide for plated nickel–copper contacts on silicon solar cells," *Solar Energy Materials and Solar Cells*, vol. 117, pp. 209–213, 2013.
12. A. Büchler *et al.*, "Interface oxides in femtosecond laser structured plated Ni-Cu-Ag contacts for silicon solar cells," *Solar Energy Materials and Solar Cells*, vol. 166, pp. 197–203, 2017.
13. H. C. Hamann *et al.*, "Electrochemistry," *Weinheim: WILEY-VCH*, 1998.
14. G. Galbiati *et al.*, "Large-area back-contact back-junction solar cell with efficiency exceeding 21%," *IEEE J. Photovoltaics*, vol. 3, no. 1, pp. 560–565, 2013.
15. G. Galbiati *et al.*, "Latest results in screen-printed IBC-ZEBRA solar cells," *IEEE 7th World Conference on Photovoltaic Energy Conversion* (WCPEC), 2018.
16. V. D. Milhalailetchi *et al.*, "A comparison study of n-type PERT and IBC Cell concepts with screen printed contacts," *Energy Procedia*, vol. 77, pp. 534–539, 2015.
17. A. Halm *et al*., "Evaluation of cell to module losses for n-type IBC solar cells assembled with state of the art consumables and production equipment," *IEEE 39th Photovoltaic Specialists Conference (PVSC),* pp. 2368-2372, 2013.